BIOCHEMICAL PHARMACOLOGY 72 (2006) 332–343

available at www.sciencedirect.com

SCIENCE DIRECT®

journal homepage: www.elsevier.com/locate/biochempharm

Gene expression profiling changes induced by a novel Gemini Vitamin D derivative during the progression of breast cancer

Hong Jin Lee [a,1], *Hao Liu* [b,1], *Catherine Goodman* [a], *Yan Ji* [a], *Hubert Maehr* [a], *Milan Uskokovic* [a], *Daniel Notterman* [b,c], *Michael Reiss* [b], *Nanjoo Suh* [a,b,*]

[a] *Department of Chemical Biology, Ernest Mario School of Pharmacy, Rutgers, The State University of New Jersey, Piscataway, NJ 08854, United States*

[b] *The Cancer Institute of New Jersey, New Brunswick, NJ 08903, United States*

[c] *Department of Pediatrics and Molecular Genetics, Robert Wood Johnson Medical School, University of Medicine and Dentistry of New Jersey, New Brunswick, NJ 08903, United States*

ARTICLE INFO

Article history:
Received 22 March 2006
Accepted 21 April 2006

Keywords:
MCF10
Breast cancer
Gemini Vitamin D_3
Bone morphogenetic protein
TGF-β
Smad3

Abbreviations:
BMP, bone morphogenetic protein
CTGF, connective tissue growth factor
IGFBP-3, insulin-like growth factor binding protein-3
JNK, C-jun N-terminal kinase
MMPs, matrix metalloproteinases
TGF-β, transforming growth factor-β
TIMPs, tissue inhibitors of matrix metalloproteinases
VDR, Vitamin D receptor

ABSTRACT

We investigated gene expression changes induced by a novel Gemini Vitamin D_3 analog, RO-438-3582 (1α,25-dihydroxy-20S-21(3-hydroxy-3-methyl-butyl)-23-yne-26,27-hexafluoro-cholecalciferol, Ro3582), in a unique human breast MCF10 model. We used two breast epithelial cell lines from this model, namely MCF10AT1 (*Ha-ras* oncogene transfected MCF10A, early premalignant) and MCF10CA1a (fully malignant and metastatic derived from the MCF10AT1 line). We analyzed gene expression changes induced by Ro3582 using GeneChip technology, quantitative RT-PCR, Western blot analysis, or a gene transcription assay. Interestingly, we found distinct gene expression profile differences between Ro3582-induced response of the early premalignant MCF10AT1 and the malignant and metastatic MCF10CA1a cell lines. Moreover, while the Gemini Vitamin D_3 analog Ro3582 modulated the expression of several Vitamin D target genes such as the 24-hydroxylase, CD14, osteocalcin, and osteopontin in both cell lines, Ro3582 regulated many genes involved in cell proliferation and apoptosis, cell adhesion, invasion, angiogenesis as well as cell signaling pathways, such as the BMP and TGF-β systems, differently in the two cell lines. The Gemini Vitamin D_3 analog Ro3582 induced more significant gene changes in the early premalignant MCF10AT1 cells than in the malignant metastatic MCF10CA1a cells, suggesting that Gemini Vitamin D_3 analogs may be more effective in preventing the progression of an early stage of breast carcinogenesis than in treating late stage breast cancer.

* *Corresponding author*. Tel.: +1 732 445 3400x226; fax: +1 732 445 0687.
E-mail address: nsuh@rci.rutgers.edu (N. Suh).

[1] These authors contributed equally to this work.

0006-2952/$ – see front matter
doi:10.1016/j.bcp.2006.04.030

1. Introduction

The hormonally active metabolite of Vitamin D_3, 1α,25$(OH)_2D_3$, functions in the maintenance of calcium/phosphate homeostasis through regulation of genes in intestine, kidney and bone, and it also controls immune cells and hormone secretion [1,2]. Most of the effects of 1α,25$(OH)_2D_3$ are mediated through the Vitamin D receptor (VDR)-regulated transcription [3,4]. The VDR is a member of the nuclear receptor superfamily, and functions as a heterodimer with the master dimerization partner, retinoid X receptor (RXR) [5]. When 1α,25$(OH)_2D_3$ or its analogs bind to the VDR, the receptor interacts with the RXR, as well as with other transcription factors including coactivators and corepressors, to activate the selective transcription of VDR-dependent genes [4].

The VDR is present in normal and lactating mammary gland, in breast tumors, and in cell lines derived from human breast cancers [6–8], and 1α,25$(OH)_2D_3$ and certain Vitamin D_3 analogs have been shown to exert potent growth inhibitory effects on breast cancer cells. For example, 1α,25$(OH)_2D_3$ and its classic synthetic analogs have been shown to induce apoptosis and to arrest the cell cycle in the G1 phase by increasing the level of cyclin-dependent kinase inhibitors, such as p21 and p27 [9,10]. In addition, 1α,25$(OH)_2D_3$ and certain Vitamin D_3 analogs have been shown to inhibit invasion, angiogenesis, and metastasis [3,10–12]. Although the growth inhibitory effect of 1α,25$(OH)_2D_3$ and several of its classic analogs in cell culture may be important for the treatment and prevention of cancer, the hypercalcemic effect of 1α,25$(OH)_2D_3$ has limited their use for the treatment and prevention of breast cancer [2]. Therefore, many different classes of synthetic Vitamin D_3 analogs have been developed to overcome the hypercalcemic toxicity. Among these, Gemini analogs of Vitamin D_3 have been reported to have considerably less toxicity than 1α,25$(OH)_2D_3$ in animals [13].

In this study, we have investigated more than 25 different Gemini analogs of Vitamin D_3 that contain two six carbon side-chains, combining a C-20-normal with a C-20-epi side chain (see Fig. 1 for some selected analogs) [14–16]. Certain Gemini analogs of Vitamin D_3 have shown low hypercalcemic toxicity profiles, due to increased metabolic stability of the analogs and different properties of the liganded VDR facilitating VDR action, resulting in more cofactor binding and elevated levels of transcription [17–19]. Although certain Gemini analogs of Vitamin D_3 were shown to treat and prevent colon cancer [13], Gemini analogs of Vitamin D_3 have not been investigated in breast cancer models.

Here, we report for the first time the effects of Gemini analogs of Vitamin D_3 on proliferation and gene expression in a unique MCF10 estrogen receptor negative breast cancer model. The series of cell lines of the MCF10 model have the same origin (MCF10A; normal immortalized). All established MCF10 breast epithelial cell lines were initiated after transfecting *Ha-ras* oncogene into MCF10A (designated as MCF10AT1), and further passaged in mice to select more aggressive and malignant cell lines [20,21]. The establishment

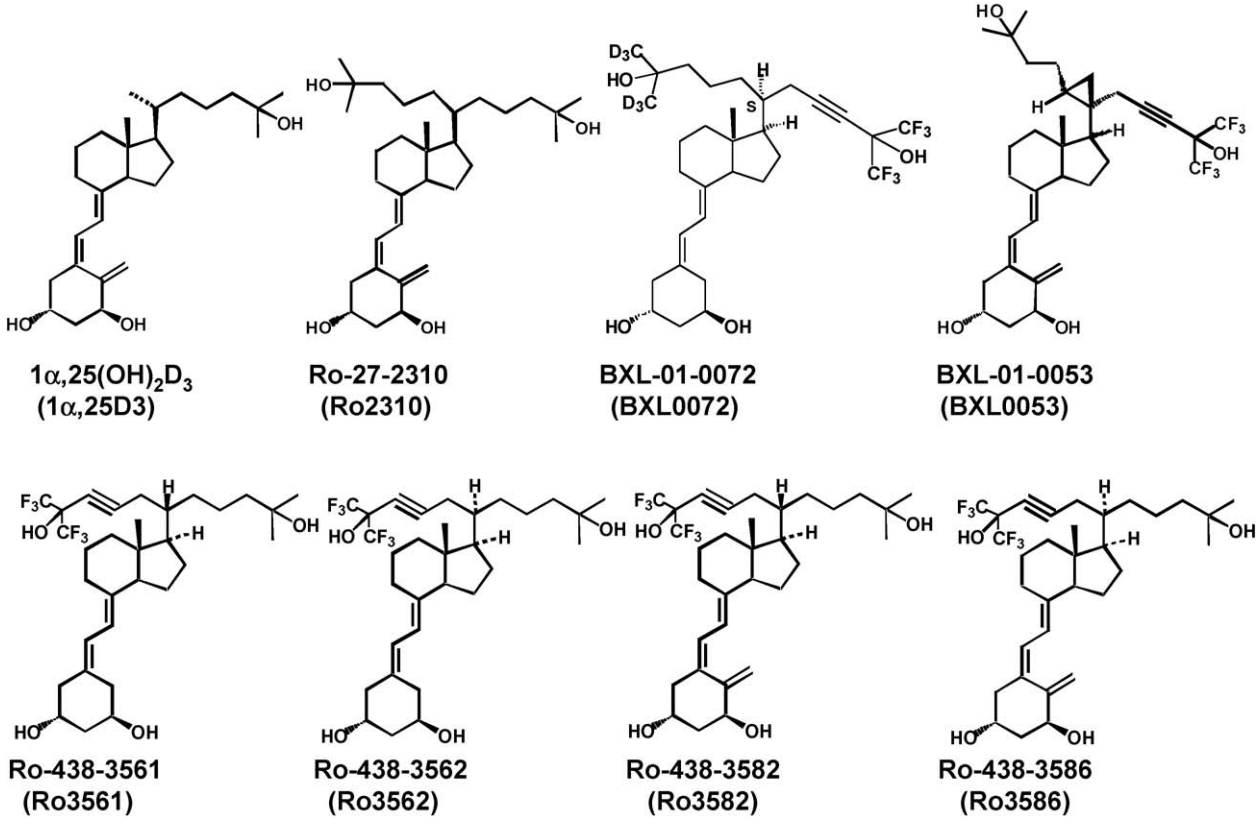

Fig. 1 – Structures of 1α,25-dihydoxyvitamin D_3 [active Vitamin D_3 metabolite, 1α,25$(OH)_2D_3$], and its synthetic Gemini Vitamin D_3 analog, RO-438-3582 (1α,25-dihydroxy-20*S*-21(3-hydroxy-3-methyl-butyl)-23-yne-26,27-hexafluoro-cholecalciferol, Ro3582). The chemical names and structures of other Gemini analogs have been reported [16,17].

of MCF10 cell lines, such as MCF10AT1 (early premalignant), MCF10DCIS (invasive potential, isolated from MCF10AT1), MCF10CA1h (aggressive malignant, isolated from MCF10AT1) or MCF10CA1a (fully malignant and metastatic, isolated from MCF10AT1), has been reported [22–24]. Among the several MCF10 cell lines available, we have tested novel Gemini Vitamin D_3 derivatives in two cell lines, MCF10AT1 (forms premalignant lesions in immunodeficient mice) and MCF10CA1a (produces undifferentiated carcinomas with metastatic potential in immunodeficient mice). Although several gene profiling studies with $1\alpha,25(OH)_2D_3$ have been reported for prostate cancer and breast cancer cell lines [25–27], gene changes in a progression model of estrogen receptor negative breast cancer by $1\alpha,25(OH)_2D_3$ or its analogs have not been investigated. We report here that a novel Gemini Vitamin D_3 analog (Ro3582; see Fig. 1 for structure) regulates gene expression differently in cell lines representing two different stages of breast cancer, namely MCF10AT1 (early premalignant) and MCF10CA1a (malignant and metastatic).

2. Materials and methods

2.1. Cell culture and reagents

2.1.1. Reagents

$1\alpha,25(OH)_2D_3$ and all Gemini Vitamin D_3 analogs including Ro3582 [1α,25-dihydroxy-20S,21(3-hydroxy-3-methylbutyl)-23-yne-26,27-hexafluorocholecalciferol] (>95% purity) were synthesized at Hoffmann-La Roche Inc. (Nutley, NJ). Fugene6 and Trizol® solution were obtained from Roche Diagnostics (Indianapolis, IN) and Invitrogen (Carlsbad, CA), respectively. $1\alpha,25(OH)_2D_3$ and Vitamin D_3 analogs were dissolved in dimethylsulfoxide (DMSO) before addition to cell cultures; final concentrations of DMSO were 0.1% or less. Controls with DMSO alone were run in all cases.

2.1.2. Cell culture

The MCF10AT1 (MCF10AT1k.clone2) and MCF10CA1a (MCF10CA1a.clone1) cell lines were established and provided by Dr. Fred Miller's group at the Barbara Ann Karmanos Cancer Institute (Detroit, MI) [20–23]. Human breast epithelial MCF10 series (including MCF10AT1 and MCF10CA1a) cell lines were grown in complete media (DMEM/F12 supplemented with 5% horse serum and 1% penicillin/streptomycin) at 37 °C, 5% CO_2. The culture medium for the MCF10AT1 cell line was the same as the medium for MCF10CA1a except it was supplemented with 10 μg/ml insulin, 20 ng/ml EGF, 0.5 μg/ml hydrocortisone, and 100 ng/ml cholera toxin.

2.2. Construction of microarray, total RNA extraction, RNA amplification and labeling, array hybridization and post-hybridization processes, scanning and data analysis

MCF10 human breast epithelial cells were treated with vehicle alone (DMSO control) or with 1 nM Vitamin D_3 analog Ro3582 for 4 and 12 h. Total RNA was isolated using the Trizol according to the manufacturer's instruction (Invitrogen, Carlsbad, CA). cDNA was synthesized with the Superscript Choice kit (Invitrogen, Carlsbad, CA). Biotin-labeled cRNA was synthesized by in vitro transcription. The cRNA was then fragmented and hybridized to a human HG-133A_2 chip (Affymetrix, Santa Clara, CA), which has 18,000 transcripts representing 14,500 genes and expressed sequence tags. The chips were washed, stained and scanned using an Affymetrix scanner. Scanned output files analyzed with the Affymetrix Gene Chip Operating Software (ver 1.1.1.052 GCOS). Signal values were determined by a one-step Tukey's biweight algorithm and normalized to a mean value of 150. To determine significant changes between treatment and control groups, ratios were calculated by GCOS, and genes with a signal level of at least 200 and that were at least two-fold higher than the control ($p < 0.003$) were selected.

2.3. [^{3}H]thymidine uptake assay

MCF10AT1 and MCF10CA1a cells were plated in 24-well plates (5000 cells/well). The cells were treated with $1\alpha,25(OH)_2D_3$ and Gemini Vitamin D_3 analogs for 3 days. One μCi of [^{3}H] thymidine was added 3 h before the harvest and the cells were analyzed with a Beckman liquid scintillation counter (Fullerton, CA).

2.4. Quantitative real-time PCR

Thirty ng of RNA was reverse transcribed to cDNA using the random primers and Applied Biosystems' High Capacity cDNA Archive Kit in a 96-well format Mastercycler Gradient from Eppendorf North America (Westbury, NY). Then, cDNA was amplified with Assays-on-Demand Products containing two gene specific primers and one TaqMan MGB probe (6-FAM dye-labeled) using the TaqMan Universal PCR Master Mix in ABI Prism 7000 Sequencing Detector (Applied Biosystems, Foster City, CA). Thermal cycling conditions were: 1 cycle of 50 °C for 2 min, 1 cycle of 95 °C for 10 min, and 40 cycles of 95 °C for 15 s and 60 °C for 1 min. GAPDH was used as an internal control and the relative changes of gene expression were calculated by the following formula, as described previously [28,29]: fold change $= 2^{-\Delta\Delta C_t} = 2^{-[\Delta C_t(\text{Ro3582 treated samples}) - \Delta C_t(\text{vehicle control})]}$, where $\Delta C_t = C_t(\text{detected gene}) - C_t(\text{GAPDH})$ and C_t = threshold cycle number.

2.5. Western blot analysis

These procedures have been described previously [30]. The primary antibodies against VDR (Affinity BioReagents, Golden, CO), actin (Sigma, St. Louis, MO), phospho-Smad1/5/8 (Cell Signaling Technology Inc., Beverly, MA), IGFBP-3 (Upstate, Lake Placid, NY), Smad3 (Zymed Laboratories Inc., South San Francisco, CA), p21, p27, and BCL-2 (Santa Cruz Biotechnology, Santa Cruz, CA), and secondary antibodies (Santa Cruz Biotechnology, Santa Cruz, CA) were used. Cells were treated with test compounds and harvested at the time indicated in the figure legends.

2.6. Plasmids and transfection assay

pCMV-β-gal and VDRE-Luc were provided by Dr. David Mangelsdorf (University of Texas Southwestern Medical School at Dallas, Texas). CYP24-Luc vectors were obtained from Dr. Sylvia Christakos (University of Medicine and

Dentistry of New Jersey, Newark, NJ); Smad3 was kindly provided by Dr. Anita Roberts (National Cancer Institute, NIH, Bethesda, MD). For transient transfection assays, cells were plated and transfected with a total of 300 ng of DNA vectors, such as VDRE-Luc, Smad3, CYP24-Luc or pCMV-β-gal. Cells were transfected using Fugene6 in serum-free medium for 6 h, and then replaced with fresh medium (0.1% BSA/DMEM) with test compounds. Twenty-four hours later, cells were washed with PBS and lysed with 100 μl of 1× reporter lysis buffer (Promega Corp., Madison, WI). Luciferase values were analyzed using Veritas Microplate Luminometer (Turner Biosystems, CA) and normalized for β-galactosidase activity.

2.7. Statistical analysis

Data analysis was performed using the comparative analysis algorithm implemented in GCOS software provided by Affymetrix (Santa Clara, CA). It generates changes in *p* values and associated changes for each probeset using Wilcoxon's signed ranked test and gene expression level changes using one-step Tukey's biweight method. We generated changes in gene expression values of the treated cell line by comparing it with the control cell line at each time point.

3. Results

3.1. Growth inhibitory effect of 1α,25-dihydroxyvitamin D_3 and the Gemini Vitamin D_3 analog Ro3582 in MCF10 breast epithelial cells

In a series of MCF10 breast epithelial cell lines, we selected MCF10AT1 cells (early premalignant) and MCF10CA1a (fully malignant and metastatic) for growth inhibition and microarray assays. However, the parental MCF10A cell line was not included because normal immortalized MCF10A cells do not have *Ha-ras* oncogene and Gemini Vitamin D_3 analogs only very weakly inhibited growth of these cells (data not shown). The growth rate of MCF10AT1 cells is similar to MCF10CA1a cells using the same medium. However, MCF10AT1 cells grow as a uniform epithelial monolayer, whereas MCF10CA1a cells grow as multiple layers.

Estrogen does not stimulate growth in either the MCF10AT1 or MCF10CA1a cell line indicating that they are estrogen non-responsive, but both cell lines express the Vitamin D receptor (VDR) determined by RT-PCR (data not shown). Therefore, we predicted that 1α,25$(OH)_2D_3$ and novel Gemini Vitamin D_3 analogs (Fig. 1) may regulate growth of these cell lines. We tested more than 25 different Gemini Vitamin D_3 analogs for their ability to inhibit cell proliferation of MCF10 breast epithelial cells. Growth inhibition by seven of these Gemini analogs are shown (up to 60–80% growth inhibition at 1 nM), and each of these Gemini analogs was more active than 1α,25$(OH)_2D_3$ at 1 nM (Fig. 2A).

Among the highly active Gemini Vitamin D_3 analogs, we selected Ro3582 to determine IC_{50} values in a dose-dependent growth inhibition assay. In MCF10AT1 cells, Ro3582 inhibited cell growth with an IC_{50} value of 0.04 nM, whereas the active Vitamin D_3 metabolite, 1α,25$(OH)_2D_3$, had an IC_{50} value of 8.2 nM. In MCF10CA1a cells, the IC_{50} values of Ro3582 and

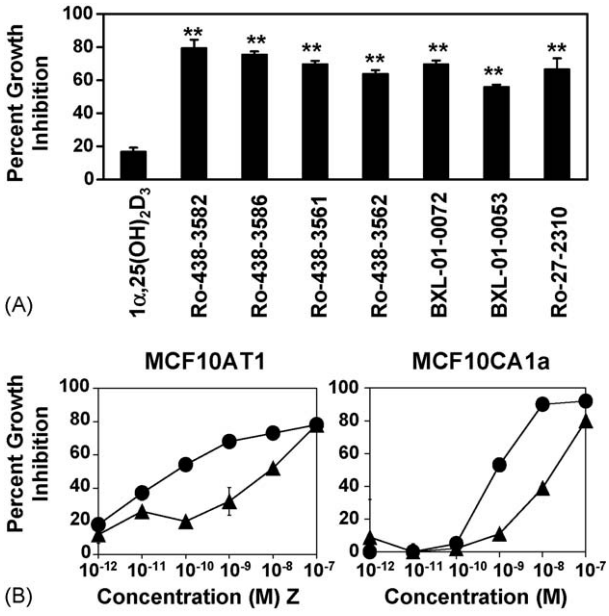

Fig. 2 – (A) Inhibition of cell proliferation by 1α,25$(OH)_2D_3$ and novel Vitamin D_3 analogs including Ro3582 in MCF10 progressive breast epithelial cells. MCF10AT1 cells were incubated with Vitamin D_3 analogs (1 nM) in 5% horse serum/DMEM/F-12 for 3 days. [^{3}H]thymidine was added, and 3 h later, incorporation of [^{3}H]thymidine into DNA was determined. Radioactivity in total DNA was measured (statistical significance, $^{**}p < 0.001$). (B) Dose-dependent inhibition of growth by 1α,25$(OH)_2D_3$ and novel Vitamin D_3 analog Ro3582 in MCF10 progressive breast epithelial cells. Cells (MCF10AT1 and MCF10CA1a) were incubated with Vitamin D_3 analogs in 5% horse serum/DMEM/F-12 for 3 days. Dose–response curves of 1α,25$(OH)_2D_3$ (triangle) and Ro3582 (circle) are shown, which are representative data from two similar experiments.

1α,25$(OH)_2D_3$ were 0.8 and 14.6 nM, respectively (Fig. 2B). In summary, many synthetic Gemini Vitamin D_3 analogs, in particular Ro3582, were at least 10–100-fold more potent than 1α,25$(OH)_2D_3$ in growth inhibition assays in these cell lines, and we selected Ro3582 for studies to determine its ability to change gene regulation in MCF10AT1 and MCF10CA1a cells.

3.2. Distinct gene expression profile differences in the responsiveness of MCF10AT1 and MCF10CA1a cells to Ro3582

We investigated the ability of Ro3582 to regulate gene expression in MCF10AT1 and MCF10CA1a cells. In our study, both cell lines were treated with Ro3582 (1 nM), and total RNA was obtained after 4 and 12 h and processed for microarray analysis. We used the comparative analysis algorithm provided in Affymetrix GCOS software to compare the effect of Ro3582 at each time point. The genes regulated by Ro3582 were determined with a two-fold change cut-off value. In MCF10AT1 cells, we determined that 100 and 271 genes were up-regulated by Ro3582 (1 nM) at 4 and 12 h, respectively, and 35 and 120 genes were down-regulated by Ro3582 at 4 and 12 h,

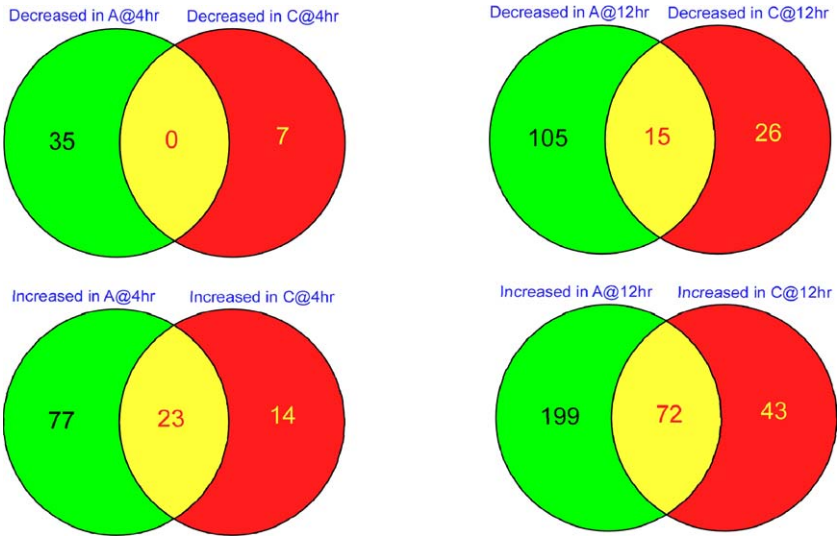

Fig. 3 – Venn diagram showing the overlap of gene profiling changes between MCF10AT1 and MCF10CA1a cells by a novel Gemini Vitamin D_3 analog Ro3582 (1 nM) at two time points (4 and 12 h). This graph shows the down-regulated gene (upper) and up-regulated gene (lower) separately. The numbers indicate the number of probesets up or down regulated at each cell line/time point combination, and green/red indicate probesets uniquely regulated, while the yellow indicate commonly regulated genes (A, MCF10AT1; C, MCF10CA1a).

respectively. In MCF10CA1a cells, we determined that 37 and 115 genes were up-regulated by Ro3582 (1 nM) at 4 and 12 h, respectively and 7 and 41 genes were down-regulated by Ro3582 at 4 and 12 h, respectively. Overall, the data showed that the Gemini Vitamin D_3 analog, Ro3582, induced more significant gene changes in the early premalignant MCF10AT1 cells than in the malignant metastatic MCF10CA1a cells.

Using the ingenuity pathway analysis provided by Ingenuity Inc. (Redwood City, CA), we analyzed the biological effects of Ro3582 with a global scale. As shown in Fig. 3, the two cell lines are different in their gene expression profile. Interestingly, many genes that are related to apoptosis and cell growth were highly regulated, but there were only a few overlapping genes (less than 20 genes) affected by Ro3582 in both cell lines. The genes showing expression changes at 4 and 12 h by Ro3582, determined by a two-fold change cut-off, are summarized in Tables 1 and 2. As predicted, several known $1\alpha,25(OH)_2D_3$ target genes, such as the 24-hydroxylase, osteocalcin, and CD14, were regulated by Ro3582 in both cell lines. In addition, Tables 1 and 2 showed that Ro3582 regulated the expression of many different sets of genes involved in cell proliferation, apoptosis, immunity, and cell adhesion, as well as ion channel and calcium metabolism/signaling pathways in MCF10AT1 and MCF10CA1a cells.

Another purpose of our study was to analyze the differential gene expression profiles among different stages of breast cancer cells, from MCF10AT1 to MCF10CA1a. We found that there were at least 200 genes with very different basal expression profiles between MCF10AT1 and MCF10CA1a cells ($p < 0.05$ by ANOVA test, data not shown). We have separated the pattern of gene expression profiles into two major groups, one with a low level in premalignant MCF10AT1 and a higher level in aggressive MCF10CA1a cell line, and the other with a high level of expression in the premalignant MCF10AT1 cell line and a lower level of expression in the aggressive MCF10CA1a cell line. Genes that have a low level of expression in premalignant MCF10AT1 and a higher level in the aggressive MCF10CA1a cell line were: osteonectin, bone marrow stromal cell antigen 2, tumor protein D52, 7-dehydrocholesterol reductase, protein phosphatase 1, lanosterol synthase, cathepsin H, cytochrome p450 51A1, stanniocalcin 1, CD44, RAS guanyl releasing protein 1, ubiquitin-activating enzyme E1C, BMP-7, and tubulin α3. Genes that have a high level of expression in premalignant MCF10AT1 and a lower level in aggressive MCF10CA1a cell line were: p21, tissue inhibitor of metalloproteinase 3 (TIMP-3), SHC transforming protein 1, TGF-β-induced, calcineurin Aα, IGFBP6, IGFBP7, mucin 1, keratins, collagenase 3 (MMP-13), proteasome 26S subunit, interleukin 1α, and HMG-box transcription factor, and metallothioneins (1H, 1X, 1f, 2A).

3.3. *Effect of Ro3582 on gene expression in MCF10 breast epithelial cells as measured by quantitative RT-PCR*

To confirm the gene expression changes by Ro3582 obtained from the microarray study, we used the same RNA samples and performed quantitative RT-PCR analyses. The results are summarized in Table 3.

3.3.1. *Vitamin D target genes*

We first confirmed the microarray data with the Vitamin D target genes, such as CYP24A1, osteocalcin, and osteopontin in these cells. Vitamin D 24-hydroxylase (CYP24A1) was the strongest responsive gene induced by Ro3582 (Tables 1 and 3). To determine the induction of CYP24 transcription by $1\alpha,25(OH)_2D_3$ and the novel Vitamin D_3 analog Ro3582, MCF10AT1 cells were transfected with a CYP24 full length vector (h24(OH)ase, −5500/−22, containing AP-1 and VDRE binding sites) or a CYP24 short length vector (h24(OH)ase, −316/−22, containing VDRE binding sites) linked to luciferase

Table 1 – Up-regulated gene expression by Vitamin D_3 analog, Ro3582, in MCF10 breast epithelial cells

GeneBank ID	Gene description	Fold change			
		AT1		CA1a	
		4 h	12 h	4 h	12 h
Vitamin D, bone, calcium metabolism					
NM_000711	Bone gamma-carboxyglutamate (gla) protein (osteocalcin) (BGLAP)	1.7	**7.0**	1.1	**2.1**
NM_001740	Calbindin 2, 29 kDa (calretinin)	1.5	**3.7**	1.1	1.4
AI093569	Calcium/calmodulin-dependent protein kinase (CaM kinase) II gamma	**2.0**	**2.0**	1.5	**2.0**
NM_001216	Carbonic anhydrase IX	−1.3	**3.5**	1.2	**3.5**
NM_000782	Cytochrome P450 family 24, subfamily A, polypeptide 1	**194.0**	**724.0**	**104.0**	**588.0**
D12620	Cytochrome P450 family 4, subfamily F, polypeptide 3	**4.0**	**10.6**	1.5	**2.0**
NM_019885	Cytochrome P450, family 26, subfamily B, polypeptide 1	**4.9**	**5.7**	**2.8**	**9.8**
NM_002963	S100 calcium binding protein A7 (psoriasin 1)	**13.0**	**34.3**	1.3	**4.9**
NM_003330	Thioredoxin reductase 1	**2.0**	**2.8**	1.5	1.5
AI023317	Thyroid hormone receptor associated protein 4	**2.1**	**3.2**	1.2	1.5
Lipid metabolism					
NM_022977	Acyl-CoA synthetase long-chain family member 4	1.9	**3.5**	1.4	1.3
AL512760	Fatty acid desaturase 1	1.1	**2.1**	1.2	**2.0**
NM_003645	Soluble carrier family 27 (fatty acid transporter), member 2	1.1	1.9	−1.1	**2.0**
Cell adhesion, extracellular matrix, cytoskeleton					
NM_003474	A disintegrin and metalloproteinase domain 12 (meltrin a)	1.1	**2.6**	1.3	**2.0**
NM_001856	Collagen, type XVI, a1	**2.3**	**3.7**	1.5	**3.0**
AF061812	Keratin 16 (focal non-epidermolytic palmoplantar keratoderma)	1.7	**3.0**	1.4	**3.7**
L25541	Laminin b3	2.1	**2.0**	**2.1**	**2.8**
NM_003461	Zyxin	1.9	**2.1**	1.6	**2.0**
Cell proliferation, apoptosis, signal transduction					
NM_001945	Diphtheria toxin receptor	**2.0**	**2.5**	1.5	**2.3**
N36770	Dual specificity phosphatase 10	**6.5**	**8.0**	**4.3**	**7.5**
NM_024530	FOS-like antigen 2	**2.8**	**2.3**	**2.1**	**2.1**
NM_005308	G protein-coupled receptor kinase 5	**2.1**	**6.1**	1.4	**3.5**
NM_001924	Growth arrest and DNA-damage-inducible a	1.7	**2.1**	1.3	1.6
NM_005261	GTP binding protein overexpressed in skeletal muscle	**4.0**	**4.6**	**4.0**	**2.1**
NM_004838	Homer homolog 3	1.5	**2.6**	1.3	**2.6**
NM_005544	Insulin receptor substrate 1	1.6	**3.7**	1.5	**6.5**
M31159	Insulin-like growth factor binding protein 3	1.6	1.9	**2.6**	**2.8**
NM_002774	Kallikrein 6 (neurosin, zyme)	**6.1**	**18.4**	**2.6**	**11.3**
NM_014751	Metastasis suppressor 1	**3.5**	**6.1**	1.1	1.7
NM_013982	Neuregulin 2	**2.5**	1.4	1.4	**2.0**
NM_006096	N-myc downstream regulated gene 1	1.1	**2.1**	1.0	1.7
NM_020529	Nuclear factor of kappa light polypeptide gene enhancer, IkB-like activity	**2.6**	**2.3**	**2.6**	**3.0**
NM_014456	Programmed cell death 4 (neoplastic transformation inhibitor)	1.3	**2.5**	1.4	**2.5**
NM_004878	Prostaglandin E synthase	1.2	1.6	1.2	**2.5**
NM_002564	Purinergic receptor P2Y, G-protein coupled, 2	**5.3**	**5.3**	**2.1**	**2.3**
NM_003028	SHB (Src homology 2 domain containing) adaptor protein B	**2.3**	1.6	1.3	1.6
BC004490	v-Fos FBJ murine osteosarcoma viral oncogene homolog	**5.3**	**3.2**	**14.9**	**39.4**
Immune response, growth factors, cytokines, inflammation					
NM_000591	CD14 antigen	**26.0**	**52.0**	**6.1**	**27.9**
NM_001784	CD97 antigen	**3.0**	**4.6**	**2.0**	**2.3**
NM_000882	Interleukin 12A	1.2	**19.7**	**2.5**	**3.5**
NM_003266	Toll-like receptor 4	1.9	**2.5**	**2.3**	1.7
NM_018643	Triggering receptor expressed on myeloid cells 1	1.4	**2.5**	1.1	**7.5**
NM_003596	Tyrosylprotein sulfotransferase 1	**2.8**	**3.7**	**2.3**	**2.3**
Transcription					
D13889	Inhibitor of DNA binding 1, dominant negative helix–loop–helix protein	1.3	1.5	1.6	**2.1**
NM_002167	Inhibitor of DNA binding 3, dominant negative helix–loop–helix protein	1.4	1.7	1.7	**2.1**
NM_002229	Jun B proto-oncogene	1.7	**2.1**	**2.0**	**2.6**
AI824012	Nuclear receptor interacting protein 1	1.6	1.9	**2.0**	**2.1**
NM_003195	Transcription elongation factor A (SII), 2	**3.0**	**16.0**	−4.6	**3.2**
NM_003447	Zinc finger protein 165	1.7	**2.1**	1.5	1.9
NM_003407	Zinc finger protein 36, C3H type homolog	**2.1**	**2.1**	1.2	1.5
TGF-β, BMP, activin, Smad signaling					
AB046845	E3 ubiquitin ligase SMURF1	1.6	**2.0**	1.1	1.4
M13436	Inhibin, beta A (activin A, activin AB alpha polypeptide)	1.3	**2.1**	1.9	**4.9**

Table 1 (*Continued*)

GeneBank ID	Gene description	Fold change			
		AT1		CA1a	
		4 h	12 h	4 h	12 h
NM_001200.1	BMP-2	1.1	**2.3**	1.9	−1.2
NM_001718	BMP-6	**2.5**	**4.0**	−3.5	−1.2
M19154.1	TGF-β2	1.3	1.4	1.5	**2.1**
Transporters, channels					
AI769688	ATPase, aminophospholipid transporter (APLT), Class I, type 8A, member 1	1.4	**9.1**	3.7	**4.6**
NM_014211	Gamma-aminobutyric acid (GABA) A receptor, pi	1.2	1.7	1.4	**2.6**
L38019	Inositol 1,4,5-triphosphate receptor, type 1	1.1	**2.0**	1.3	**2.8**
AF053755	Solute carrier family 4, member 7	**2.5**	**7.0**	1.7	**3.5**
NM_016354	Solute carrier organic anion transporter family, member 4A1	1.4	**2.3**	1.5	**2.1**
NM_015993	Transmembrane 4 superfamily member 11 (plasmolipin)	1.6	**4.3**	−1.1	**2.5**
Others					
NM_024734	Calmin (calponin-like, transmembrane)	**2.5**	**4.6**	1.9	**2.8**
NM_001873	Carboxypeptidase E	1.5	**7.0**	−1.1	**4.3**
U19970	Cathelicidin antimicrobial peptide (LPS binding protein)	**9.2**	**19.7**	**7.0**	**22.6**
BF514079	Kruppel-like factor 4 (gut)	**2.5**	**3.7**	1.5	**2.8**
NM_016233	Peptidyl arginine deiminase, type III	**8.6**	**45.3**	**2.0**	**4.0**
AI554300	Serine (or cysteine) proteinase inhibitor, clade B (ovalbumin), member 1	**4.6**	**12.1**	**2.3**	**9.2**
U90902	T-cell lymphoma invasion and metastasis 1	**2.6**	**2.8**	**2.0**	**2.6**
BE676218	Three prime repair exonuclease 2	1.4	**2.0**	1.3	**2.3**
NM_000930	Tissue plasminogen activator (tPA)	**2.0**	**2.0**	**2.0**	**2.3**
NM_003282	Troponin I, skeletal, fast	1.4	1.5	**2.1**	**9.8**

Bold indicates more than two-fold changes.

Table 2 – Down-regulated gene expression by Vitamin D_3 analog, Ro3582, in MCF10 breast epithelial cells

GeneBank ID	Gene description	Fold change			
		AT1		CA1a	
		4 h	12 h	4 h	12 h
Cell adhesion, extracellular matrix, cytoskeleton					
NM_003246	Thrombospondin 1	−1.4	**−2.0**	−1.3	−1.6
NM_002291	Laminin b1	−1.5	**−2.3**	−1.2	−1.9
X16354	Carcinoembryonic antigen-related cell adhesion molecule 1	−1.3	**−3.5**	−1.1	**−2.5**
NM_001723	Bullous pemphigoid antigen 1	−1.5	**−2.0**	−1.3	**−2.8**
BF196457	Desmocollin 2	−1.6	**−2.0**	−1.4	−1.5
AF307080	Latrophilin 3	−1.1	**−3.2**	−1.1	−1.9
Signal transduction, apoptosis, cell cycle					
NM_003507	Frizzled homolog 7	−1.3	**−2.5**	−1.6	**−2.3**
NM_002048	Growth arrest-specific 1	**−3.2**	**−3.5**	−1.9	**−2.8**
NM_003897	Immediate early response 3	−1.5	−2.5	−1.1	−1.3
NM_000676	Adenosine A2b receptor	−1.4	−2.3	−1.2	−1.3
Growth factors, cytokines, immune responses, inflammation					
NM_005582	Lymphocyte antigen 64 homolog, radioprotective	−1.8	**−4.9**	−1.8	**−6.5**
M92934	Connective tissue growth factor (CTGF)	−1.9	**−2.6**	2.3	**−3.0**
Transcription					
NM_005375	v-myb myeloblastosis viral oncogene homolog	**−2.3**	−1.9	−1.5	−1.7
AI572079	Snail homolog 2 (SNAI2)	−1.2	−1.5	**−2.3**	**−4.0**
Others					
NM_005077	Transducin-like enhancer of split 1	−1.6	**−2.3**	−1.4	**−2.0**
NM_001218	Carbonic anhydrase XII	1.0	−1.7	−1.2	**−2.8**
NM_004385	Chondroitin sulfate proteoglycan 2 (versican)	−1.5	**−2.5**	−1.1	−1.7

Bold indicates more than two-fold changes.

Table 3 – Validation of microarray analyses by quantitative RT-PCR

Gene description	Fold change			
	AT1		CA1a	
	4 h	12 h	4 h	12 h
Vitamin D target genes				
CYP24A1	**6028 ± 310**	**7523 ± 162**	**462 ± 54**	**4144 ± 95**
Osteocalcin	**80.7 ± 2.5**	**279 ± 71**	**9.2 ± 1.8**	**56.2 ± 5.8**
Osteopontin	**7.0 ± 1.2**	**30.1 ± 10.1**	1.5 ± 0.8	**6.6 ± 0.4**
Vitamin D receptor (VDR)	1.0 ± 0.3	1.4 ± 0.2	1.1 ± 0.2	1.3 ± 0.1
Cell adhesion, invasion, angiogenesis, and metastasis				
Collagen, type XVI, α1	**2.5 ± 0.0**	**3.9 ± 0.1**	1.4 ± 0.1	**2.2 ± 0.5**
Laminin β3	**2.7 ± 0.5**	**3.0 ± 0.2**	**2.2 ± 0.2**	**3.7 ± 0.1**
Thrombospondin 1	−1.7 ± 0.3	**−2.4 ± 0.8**	−1.5 ± 0.1	−1.7 ± 0.0
Laminin β1	−1.3 ± 0.2	**−2.3 ± 0.5**	−1.4 ± 0.1	**−2.4 ± 0.1**
MMP-1	**2.1 ± 0.6**	**9.4 ± 2.8**	0.8 ± 0.0	1.8 ± 0.7
MMP-2	−1.1 ± 0.1	**−3.0 ± 0.1**	−1.3 ± 0.5	**−2.5 ± 0.7**
Connective tissue growth factor (CTGF)	**−2.1 ± 0.1**	**−2.2 ± 0.0**	1.0 ± 0.2	**−5.0 ± 0.3**
Cell growth, apoptosis, and signal transduction				
Insulin receptor substrate 1	1.9 ± 0.1	**3.6 ± 0.7**	1.3 ± 0.1	**6.4 ± 1.6**
Insulin-like growth factor binding protein 3	1.5 ± 0.1	**2.2 ± 0.2**	**2.7 ± 0.3**	**3.0 ± 0.2**
Dual specificity phosphatase 10	**10.3 ± 2.8**	**10.4 ± 0.5**	**4.1 ± 0.0**	**8.8 ± 1.4**
p21	1.2 ± 0.6	1.3 ± 0.1	0.8 ± 0.1	0.7 ± 0.1
p27	0.8 ± 0.2	1.0 ± 0.0	0.9 ± 0.1	0.7 ± 0.0
BCL-2	−0.9 ± 0.0	−1.3 ± 0.1	−1.6 ± 0.1	−1.2 ± 0.2
Transcription				
Snail homolog 2 (SNAI2)	−1.3 ± 0.3	**−2.0 ± 0.1**	**−2.1 ± 0.8**	**−4.5 ± 1.2**
TGF-β/BMP signaling				
BMP-2	**2.0 ± 0.2**	**2.6 ± 0.0**	1.5 ± 0.1	**2.3 ± 0.7**
BMP-6	**4.6 ± 1.0**	**8.0 ± 2.7**	1.1 ± 0.1	1.8 ± 0.3
BMP-7	–	–	0.8 ± 0.0	0.7 ± 0.1
Inhibin, beta A (activin A)	1.4 ± 0.1	1.9 ± 0.2	**2.0 ± 0.6**	**4.1 ± 0.4**
TGF-β2	1.5 ± 0.1	0.9 ± 0.2	1.7 ± 0.8	1.3 ± 0.1
TGF-β receptor II	1.3 ± 0.3	1.4 ± 0.1	1.1 ± 0.1	0.9 ± 0.1
Smad6	**−3.3 ± 0.0**	**−2.1 ± 0.0**	**−2.4 ± 0.3**	**−4.4 ± 0.7**
Smad7	1.0 ± 0.3	1.4 ± 0.1	0.8 ± 0.1	0.7 ± 0.1
E3 ubiquitin ligase SMURF1	1.3 ± 0.3	1.4 ± 0.4	0.9 ± 0.2	1.2 ± 0.2

Bold indicates more than two-fold changes. Each value represents the mean ± S.E. from two separate experiments.

[31]. The CYP24 gene transcription was induced by $1\alpha,25(OH)_2D_3$, but increased more significantly by Ro3582 at the concentrations of 0.01, 0.1, and 1 nM (Fig. 4A). In addition, we transfected MCF10AT1 cells with a VDRE-luc alone or together with Smad3. We found that Ro3582 induced the transactivation of the VDR response to a much greater extent than $1\alpha,25(OH)_2D_3$ in the presence of the transfected Smad3, a known coactivator for the VDR response (Fig. 4B).

3.3.2. *Cell adhesion, invasion, angiogenesis, and metastasis*

We found that Ro3582 regulated cell adhesion molecules, such as collagens, laminins, thrombospondin, keratin and zyxin (Tables 1 and 2). Among them, we confirmed that collagen type XVIα1 and laminin β3 were up-regulated, while thrombospondin-1 and laminin β1 were down-regulated by Ro3582 (Table 3). Interestingly, one of the MMPs, MMP-2, which is known to be involved in invasion, was down regulated by Ro3582 in both MCF10AT1 and MCF10CA1a cells, whereas the expression of MMP-1 was induced in MCF10AT1 cells (Table 3). The expression of an angiogenic marker, connective tissue growth factor (CTGF), was inhibited by Ro3582 in both MCF10AT1 and MCF10CA1a cell lines (Table 3).

3.3.3. *Cell growth, apoptosis and signal transduction*

IGFBP-3 (Insulin-like growth factor binding protein-3) has been shown to play a key role in the growth arrest induced by $1\alpha,25(OH)_2D_3$ [32]. Here, we showed that insulin receptor substrate 1 and IGFBP-3 were both up-regulated by Ro3582 (Table 3). Furthermore, dual specificity phosphatase 10, a member of the MAPK superfamily, which is known to be a negative regulator of proliferation, was highly up-regulated by Ro3582 in MCF10AT1 and MCF10CA1a cells. The gene expression changes of p21, p27 or BCL-2 induced by Ro3582 were less than two-fold when determined by quantitative RT-PCR (Table 3).

3.3.4. *The TGF-β superfamily*

In the microarray analysis, Ro3582 induced the expression of BMP-2, BMP-6 and activin A in MCF10AT1 cells, whereas BMP-2 and BMP-6 were down regulated by Ro3582 in MCF10CA1a cells (Table 1). However, using quantitative RT-PCR, we confirmed that BMP-2, BMP-6 and activin A were up-regulated in both cell lines. Furthermore, Smad6, an inhibitory Smad of BMP signaling, was down-regulated by Ro3582 in both cell lines (Table 3).

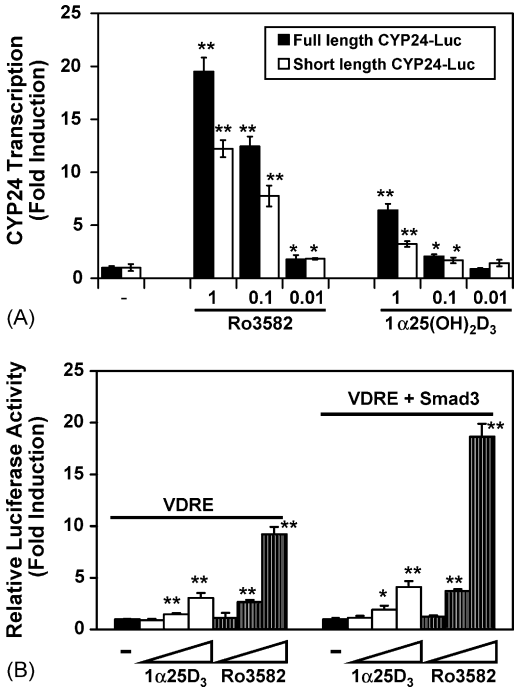

Fig. 4 – (A) Induction of CYP24 transcription by 1α,25(OH)$_2$D$_3$ and the novel Vitamin D$_3$ analog Ro3582 in MCF10AT1 cells. Cells were transfected with a CYP24 full length vector (h24(OH)ase, −5500/−22) or a CYP24 short length vector (h24(OH)ase, −316/−22) linked to luciferase using Fugene6 in serum-free media. Six hours later, the cells were treated with compounds (nM) in 0.1% BSA/DMEM/F-12 medium and incubated for 24 h. Luciferase assay was performed using a 96-well plate in a luminometer, and the value was normalized for β-galactosidase activity (statistical significance, $^{*}p < 0.05$, $^{**}p < 0.001$). (B) Interaction of the Vitamin D receptor and Smad3 is induced by the Gemini Vitamin D$_3$ analog, Ro3582, in MCF10AT1 cells. Cells were transfected with VDRE-luc (50 ng), and/or Smad3 (50 ng) using Fugene6 in serum-free media. Six hours later, cells were treated with 1α,25(OH)$_2$D$_3$ (1α,25D$_3$, 1, 10, 100 pM) or Ro3582 (1, 10, 100 pM) in 0.1% BSA/DMEM/F-12 medium for 24 h (statistical significance, $^{*}p < 0.05$, $^{**}p < 0.001$).

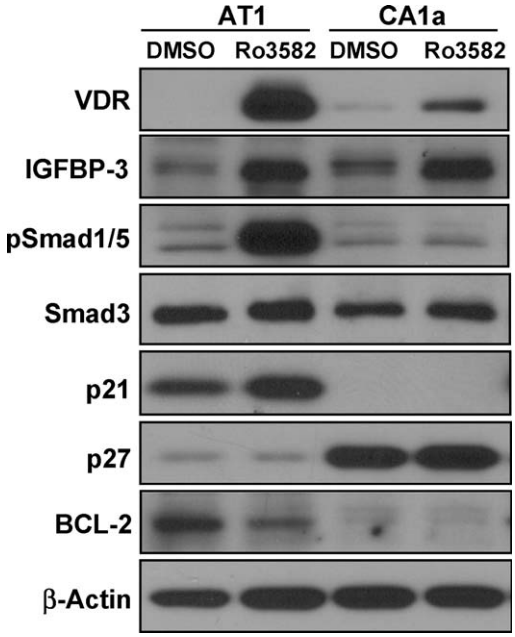

Fig. 5 – Regulation of protein expression by Gemini Vitamin D$_3$ analog Ro3582 in MCF10AT1 and MCF10CA1a breast epithelial cells. MCF10AT1 and MCF10CA1a cells (5×10^5 cells/6-well plate) were starved for 24 h in serum-free DMEM/F-12 medium. Then, cells were incubated with DMSO or Ro3582 (10 nM) in 0.1% BSA/DMEM/F-12 medium for 24 h before protein harvest.

3.4. *Effect of Ro3582 on protein levels in MCF10 breast epithelial cells*

Because the regulation at the mRNA level does not always predict regulation at the protein level, we investigated the effects of Ro3582 on expression levels of several proteins by Western blot analysis (Fig. 5). First, we determined the induction of the VDR protein expression by Ro3582. Although Ro3582 induced the VDR protein expression in both cell lines, induction of the VDR protein in MCF10AT1 cells was much stronger than in MCF10CA1a. In addition, we analyzed several key proteins that are known to regulate cell growth and apoptosis, such as IGFBP-3, p21, p27, and BCL-2, in both cell lines. We found that the level of IGFBP-3 was increased substantially by Ro3582 in both cell lines. Interestingly, Ro3582 induced the expression of p21 protein in MCF10AT1 cells, whereas the expression of p21 protein is completely lost in MCF10CA1a cells. In contrast, MCF10CA1a cells have a much higher basal level of p27 than MCF10AT1 cells, but Ro3582 did not change the protein level of p27 in either cell line. In addition, the level of anti-apoptotic protein, BCL-2, was decreased by Ro3582 in MCF10AT1, but it was not detected in MCF10CA1a cells (Fig. 5). Since Ro3582 regulated the expression of the members of the TGF-β/BMP signaling pathway, we also determined the level of phosphorylation of Smad1/5, which is known to be phosphorylated by active BMP-receptor kinase. The level of phospho-Smad1/5 was strongly increased by the treatment with Ro3582 in MCF10AT1 cells, while it was not changed in MCF10CA1a cells. Smad3 protein levels are also shown in both cell lines (Fig. 5).

4. Discussion

In the present study, we utilized an oligo microarray approach to evaluate changes in the gene expression profile after treatment of MCF10AT1 and MCF10CA1a cell lines with the Gemini Vitamin D$_3$ analog, Ro3582. Although several studies have shown gene expression profile changes after treatment with 1α,25(OH)$_2$D$_3$ in prostate, colon, ovarian, and breast cancer cells [25–27,33–38], our study is unique because it reports on the effect of a novel Gemini Vitamin D$_3$ analog on gene expression in an estrogen receptor negative breast cancer progression model. The cells studied were MCF10AT1 (early premalignant cell line) and MCF10CA1a (aggressive

metastatic cell line). While MCF10AT1 cells form premalignant lesions or occasionally develop tumors when they are injected into immunodeficient mice, MCF10CA1a cells always and rapidly form undifferentiated carcinomas in mice [24].

A recent study with carcinogen-transformed MCF-12F breast epithelial cells has shown that the growth inhibitory effect of a Vitamin D analog $1\alpha(OH)D_5$ was achieved in precancerous or cancer cells but was found to be ineffective in normal-like MCF-12F breast epithelial cell line [39]. Using MCF10 cell lines, we also found that Gemini Vitamin D_3 analogs did not significantly inhibit growth of normal immortalized breast epithelial MCF10A cells. However, Gemini Vitamin D_3 analogs have growth inhibitory effects in both premalignant MCF10AT1 and malignant MCF10CA1a cells.

In both breast epithelial cell lines, the most responsive gene identified was human CYP24 (24-hydroxylase). CYP24 is an enzyme involved in the deactivation of $1\alpha,25(OH)_2D_3$ to an inactive metabolite by adding a hydroxyl group to the C24 position. This induction was confirmed by both quantitative RT-PCR and CYP24 transcription assays. Other known Vitamin D target genes such as osteopontin, osteocalcin and CD14 were also highly induced by the Gemini Vitamin D_3 analog Ro3582. Both the present study with Ro3582 and previously reported studies with $1\alpha,25(OH)_2D_3$ [26,27,33–35,40] show that many genes related to cell growth and cell adhesion/matrix proteins are regulated by treatment with $1\alpha,25(OH)_2D_3$ or a Gemini analog. Genes reported to be regulated by $1\alpha,25(OH)_2D_3$ in different cell types were also affected by Ro3582 in MCF10AT1 and MCF10CA1a breast epithelial cells. Those genes are insulin-like growth factor binding protein 3 (IGFBP-3), thioredoxin reductase 1, zyxin, kallikrein 6, G-protein-coupled receptor kinase 5, bone morphogenetic protein 6 (BMP-6), transforming growth factor β2 (TGF-β2) and dual specificity phosphatase 10 [26,27,33–35,37,40].

It was previously reported that Smad3, a member of the TGF-β/Smad superfamily, acts as a co-activator for the Vitamin D receptor in the nucleus [41]. We show here that Ro3582 induces the transactivation of the VDR response to a much greater extent than $1\alpha,25(OH)_2D_3$ in the presence of Smad3 (Fig. 4B), suggesting that Ro3582 enhanced the interaction between Smad3 and VDR much more efficiently than $1\alpha,25(OH)_2D_3$. Previously, we found that Ro3582 enhanced phosphorylation of BMP specific Smads (Smad1/5) and activated the BMP/Smad signaling by induction of BMP-2 and BMP-6 expression in MCF10AT1 cells [42]. In this study, Ro3582 strongly induced phospho-Smad1/5 in early premalignant MCF10AT1 cells but it did not affect phospho-Smad1/5 levels in malignant MCF10CA1a cells. Although BMPs have mainly been known to stimulate bone formation, they are now identified as multifunctional molecules regulating growth, differentiation, and apoptosis in many target cells [43]. The biological effects and mechanisms by which BMPs function in breast cancer cells have not been well defined, and further investigation on the regulation of the BMP signaling pathway activated by novel Gemini Vitamin D_3 analogs in breast cancer progression might be interesting.

We analyzed the differential gene expression profiles among different stages of breast cancer cells, from MCF10AT1 to MCF10CA1a, and found that there were at least 200 genes with very different basal expression profiles between MCF10AT1 and MCF10CA1a cells. Among these genes, metallothioneins are known to constitute the majority of intracellular protein thiols and act as cell survival factors. Therefore, lower levels of metallothioneins in MCF10CA1a cells may be correlated with the higher levels of spontaneous apoptosis observed in these cells (unpublished). In accord with these observations, the level of anti-apoptotic protein BCL-2 was not detectable in MCF10CA1a cells, while MCF10AT1 cells have higher basal level of BCL-2 protein, which was significantly reduced by Ro3582 (Fig. 5). Interestingly, when we compared p21 in both cell lines, the expression of p21 protein was not detectable in MCF10CA1a cells. The opposite was shown with p27 protein expression that there was a much higher level of p27 in MCF10CA1a cells than in MCF10AT1 cells. It is possible that the loss of p21 in aggressive metastatic MCF10CA1a cells may, in part, contribute to its malignant phenotype.

In summary, we investigated the effects of a novel Gemini Vitamin D_3 analog in a unique human breast cancer progression model. We found that MCF10AT1 cells were more responsive to Ro3582 in inducing gene expression changes than MCF10CA1a cells. In addition, we also found that there were distinct gene expression profile differences between the early premalignant MCF10AT1 and the aggressive/metastatic MCF10CA1a cell lines. Unpublished in vivo data from our laboratory and studies by other investigators using a colon cancer model with Gemini analogs [13] indicate better toxicity/safety profiles for the Gemini analogs than for $1\alpha,25(OH)_2D_3$ in animals. The results of our studies suggest that Gemini Vitamin D_3 analogs may be useful drugs for the prevention of breast cancer progression. Further investigations are needed to determine the significance of gene expression changes induced by $1\alpha,25(OH)_2D_3$ and its Gemini analogs in vivo where multicellular context may play a critical role in carcinogenesis

Acknowledgments

This work was supported by NIH K22 CA 99990, NIH R03 CA112642, and a CINJ new investigator award to N.S, and Cancer Center Support Grant (5 P30 CA 072720-10) to D.N. We thank Dr. Allan Conney for helpful advice on our work. The MCF10 cell lines were established and provided by Dr. Fred Miller's group at the Karmanos Cancer Institute. The authors thank the Department of Chemical Biology and Shared Microarray Resource at the Cancer Institute of New Jersey for technical help with this project.

REFERENCES

[1] Holick MF. Sunlight and Vitamin D for bone health and prevention of autoimmune diseases, cancers, and cardiovascular disease. Am J Clin Nutr 2004;80:1678S–88S.
[2] Nagpal S, Na S, Rathnachalam R. Noncalcemic actions of Vitamin D receptor ligands. Endocr Rev 2005;26:662–87.
[3] Welsh J. Vitamin D and breast cancer: insights from animal models. Am J Clin Nutr 2004;80:1721S–4.
[4] MacDonald PN, Baudino TA, Tokumaru H, Dowd DR, Zhang C. Vitamin D receptor and nuclear receptor coactivators: crucial interactions in Vitamin D-mediated transcription. Steroids 2001;66:171–6.

[5] Mangelsdorf DJ, Evans RM. The RXR heterodimers and orphan receptors. Cell 1995;83:841–50.
[6] Eisman JA, Suva LJ, Sher E, Pearce PJ, Funder JW, Martin TJ. Frequency of 1,25-dihydroxyvitamin D3 receptor in human breast cancer. Cancer Res 1981;41:5121–4.
[7] Buras RR, Schumaker LM, Davoodi F, Brenner RV, Shabahang M, Nauta RJ, et al. Vitamin D receptors in breast cancer cells. Breast Cancer Res Treat 1994;31:191–202.
[8] Welsh J, Wietzke JA, Zinser GM, Smyczek S, Romu S, Tribble E, et al. Impact of the Vitamin D3 receptor on growth-regulatory pathways in mammary gland and breast cancer. J Steroid Biochem Mol Biol 2002;83:85–92.
[9] Narvaez CJ, Zinser G, Welsh J. Functions of 1alpha, 25-dihydroxyvitamin D(3) in mammary gland: from normal development to breast cancer. Steroids 2001;66:301–8.
[10] Flanagan L, Packman K, Juba B, O'Neill S, Tenniswood M, Welsh J. Efficacy of Vitamin D compounds to modulate estrogen receptor negative breast cancer growth and invasion. J Steroid Biochem Mol Biol 2003;84:181–92.
[11] Nakagawa K, Sasaki Y, Kato S, Kubodera N, Okano T. 22-Oxa-1alpha,25-dihydroxyvitamin D3 inhibits metastasis and angiogenesis in lung cancer. Carcinogenesis 2005;26:1044–54.
[12] Lamprecht SA, Lipkin M. Chemoprevention of colon cancer by calcium, Vitamin D and folate: molecular mechanisms. Nat Rev Cancer 2003;3:601–14.
[13] Spina C, Tangpricha V, Yao M, Zhou W, Wolfe MM, Maehr H, et al. Colon cancer and solar ultraviolet B radiation and prevention and treatment of colon cancer in mice with Vitamin D and its Gemini analogs. J Steroid Biochem Mol Biol 2005;97:111–20.
[14] Herdick M, Bury Y, Quack M, Uskokovic MR, Polly P, Carlberg C. Response element and coactivator-mediated conformational change of the Vitamin D(3) receptor permits sensitive interaction with agonists. Mol Pharmacol 2000;57:1206–17.
[15] Norman AW, Manchand PS, Uskokovic MR, Okamura WH, Takeuchi JA, Bishop JE, et al. Characterization of a novel analogue of 1alpha,25(OH)(2)-Vitamin D(3) with two side chains: interaction with its nuclear receptor and cellular actions. J Med Chem 2000;43:2719–30.
[16] Maehr H, Uskokovic MR, Reddy GS, Adorini L. Calcitriol derivatives with two different side chains at C-20. 24-Hydroxy derivatives as metabolic products and molecular probes for VDR exploration. J Steroid Biochem Mol Biol 2004;89/90:35–8.
[17] Bury Y, Herdick M, Uskokovic MR, Carlberg C. Gene regulatory potential of 1alpha,25-dihydroxyvitamin D(3) analogues with two side chains. J Cell Biochem Suppl 2001;(Suppl 36):179–90.
[18] Vaisanen S, Perakyla M, Karkkainen JI, Uskokovic MR, Carlberg C. Structural evaluation of the agonistic action of a Vitamin D analog with two side chains binding to the nuclear Vitamin D receptor. Mol Pharmacol 2003;63:1230–7.
[19] Weyts FA, Dhawan P, Zhang X, Bishop JE, Uskokovic MR, Ji Y, et al. Novel Gemini analogs of 1alpha,25-dihydroxyvitamin D(3) with enhanced transcriptional activity.. Biochem Pharmacol 2004;67:1327–36.
[20] Miller FR, Soule HD, Tait L, Pauley RJ, Wolman SR, Dawson PJ, et al. Xenograft model of progressive human proliferative breast disease. J Natl Cancer Inst 1993;85:1725–32.
[21] Miller FR, Santner SJ, Tait L, Dawson PJ. MCF10DCIS.com xenograft model of human comedo ductal carcinoma in situ. J Natl Cancer Inst 2000;92:1185–6.
[22] Strickland LB, Dawson PJ, Santner SJ, Miller FR. Progression of premalignant MCF10AT generates heterogeneous malignant variants with characteristic histologic types and immunohistochemical markers. Breast Cancer Res Treat 2000;64:235–40.
[23] Santner SJ, Dawson PJ, Tait L, Soule HD, Eliason J, Mohamed AN, et al. Malignant MCF10CA1 cell lines derived from premalignant human breast epithelial MCF10AT cells. Breast Cancer Res Treat 2001;65:101–10.
[24] Tang B, Vu M, Booker T, Santner SJ, Miller FR, Anver MR, et al. TGF-beta switches from tumor suppressor to prometastatic factor in a model of breast cancer progression. J Clin Invest 2003;112:1116–24.
[25] Swami S, Raghavachari N, Muller UR, Bao YP, Feldman D. Vitamin D growth inhibition of breast cancer cells: gene expression patterns assessed by cDNA microarray. Breast Cancer Res Treat 2003;80:49–62.
[26] Palmer HG, Sanchez-Carbayo M, Ordonez-Moran P, Larriba MJ, Cordon-Cardo C, Munoz A. Genetic signatures of differentiation induced by 1alpha,25-dihydroxyvitamin D3 in human colon cancer cells. Cancer Res 2003;63: 7799–806.
[27] Krishnan AV, Shinghal R, Raghavachari N, Brooks JD, Peehl DM, Feldman D. Analysis of Vitamin D-regulated gene expression in LNCaP human prostate cancer cells using cDNA microarrays. Prostate 2004;59:243–51.
[28] Livak KJ, Schmittgen TD. Analysis of relative gene expression data using real-time quantitative PCR and the 2(−Delta Delta C(T)) method. Methods 2001;25:402–8.
[29] Ariani F, Mari F, Pescucci C, Longo I, Bruttini M, Meloni I, et al. Real-time quantitative PCR as a routine method for screening large rearrangements in Rett syndrome: report of one case of MECP2 deletion and one case of MECP2 duplication. Hum Mutat 2004;24:172–7.
[30] Suh N, Roberts AB, Birkey Reffey S, Miyazono K, Itoh S, ten Dijke P, et al. Synthetic triterpenoids enhance transforming growth factor beta/Smad signaling. Cancer Res 2003;63:1371–6.
[31] Barletta F, Dhawan P, Christakos S. Integration of hormone signaling in the regulation of human 25(OH)D3 24-hydroxylase transcription. Am J Physiol Endocrinol Metab 2004;286:E598–608.
[32] Peng L, Malloy PJ, Feldman D. Identification of a functional Vitamin D response element in the human insulin-like growth factor binding protein-3 promoter. Mol Endocrinol 2004;18:1109–19.
[33] Katayama ML, Pasini FS, Folgueira MA, Snitcovsky IM, Brentani MM. Molecular targets of 1,25(OH)2D3 in HC11 normal mouse mammary cell line. J Steroid Biochem Mol Biol 2003;84:57–69.
[34] Peehl DM, Shinghal R, Nonn L, Seto E, Krishnan AV, Brooks JD, et al. Molecular activity of 1,25-dihydroxyvitamin D3 in primary cultures of human prostatic epithelial cells revealed by cDNA microarray analysis. J Steroid Biochem Mol Biol 2004;92:131–41.
[35] Guzey M, Luo J, Getzenberg RH. Vitamin D3 modulated gene expression patterns in human primary normal and cancer prostate cells. J Cell Biochem 2004;93:271–85.
[36] Eelen G, Verlinden L, Van Camp M, Mathieu C, Carmeliet G, Bouillon R, et al. Microarray analysis of 1alpha,25-dihydroxyvitamin D3-treated MC3T3-E1 cells. J Steroid Biochem Mol Biol 2004;89/90:405–7.
[37] Zhang X, Li P, Bao J, Nicosia SV, Wang H, Enkemann SA, et al. Suppression of death receptor-mediated apoptosis by 1,25-dihydroxyvitamin D3 revealed by microarray analysis. J Biol Chem 2005;280:35458–6.
[38] Moreno J, Krishnan AV, Feldman D. Molecular mechanisms mediating the anti-proliferative effects of Vitamin D in prostate cancer. J Steroid Biochem Mol Biol 2005;97:31–6.
[39] Hussain-Hakimjee EA, Peng X, Mehta RR, Mehta RG. Growth inhibition of carcinogen-transformed MCF-12F breast epithelial cells and hormone-sensitive BT-474 breast cancer cells by 1alpha-hydroxyvitamin D5. Carcinogenesis 2006;27:551–9.

[40] Swami S, Krishnan AV, Peehl DM, Feldman D. Genistein potentiates the growth inhibitory effects of 1,25-dihydroxyvitamin D3 in DU145 human prostate cancer cells: role of the direct inhibition of CYP24 enzyme activity. Mol Cell Endocrinol 2005;241:49–61.
[41] Yanagisawa J, Yanagi Y, Masuhiro Y, Suzawa M, Watanabe M, Kashiwagi K, et al. Convergence of transforming growth factor-beta and Vitamin D signaling pathways on SMAD transcriptional coactivators. Science 1999;283:1317–21.
[42] Lee HJ, Wislocki A, Goodman C, Ji Y, Ge R, Maehr H, et al. A novel Vitamin D derivative activates bone morphogenetic protein (BMP) signaling in MCF10 breast epithelial cells. Mol Pharmacol, 2006;69(6), in press.
[43] Miyazono K, Maeda S, Imamura T. BMP receptor signaling: transcriptional targets, regulation of signals, and signaling cross-talk. Cytokine Growth Factor Rev 2005;16:251–63.